Study on the preparation and properties of polyamide/chitosan nanocomposite fabricated by electrospinning method

Mahyar Fazeli (m.fazeli@metalmat.ufrj.br)
Universidade Federal do Rio de Janeiro
Faegheh Fazeli
Isfahan University of Medical Sciences
Tamrin Nuge
University of Nottingham - Ningbo China
Omid Abdoli
Islamic Azad University
Shokooh Moghaddam
Islamic Azad University

Research Article

Keywords: Chitosan, nanocomposite, electrospinning, polyamide, electrical properties.

Posted Date: June 22nd, 2021

DOI: https://doi.org/10.21203/rs.3.rs-241685/v1

Version of Record: A version of this preprint was published at Journal of Polymers and the Environment on July 6th, 2021. See the published version at https://doi.org/10.1007/s10924-021-02229-9.

Abstract

The principal intention of this work is to fabricate and characterize the polyamide/chitosan nanocomposite by a novel single solvent method through the electrospinning procedure. The thermal properties and morphology of prepared nanocomposite are studied by thermogravimetric analysis (TGA) and field-emission scanning electron microscopy (FE-SEM). TGA exposed that the primary decomposition temperature is reduced with rising of chitosan content in the nanocomposites and origin disintegration temperature for polyamide/chitosan nanocomposites is perceived to be in the range from 300 to 500°C. Also, FE-SEM images demonstrated that the nanofibers of chitosan have good adhesion on the matrix and are well-oriented. Besides, the crystallinity and structural characteristics of the polyamide/chitosan nanocomposites are investigated by using X-ray diffraction (XRD) and Fourier transform-infrared spectroscopy (FT-IR), respectively. The results of XRD proved that the successful blending of chitosan in polyamide is achieved via the electrospinning method. FT-IR results demonstrate that the nanofibers are consist of amine groups. Also, the electrical properties of the nanocomposite improved with the increasing content of chitosan and the conductivity of the polyamide/chitosan 5 wt% demonstrates the maximum current of 0.3 nA. Besides, the sheet resistance of the composite reduced 118 to 20×10^9 Ω with raising the chitosan volume from 0 to 5 wt%.

1. Introduction

Application, supply, and demand for biodegradable materials from renewable sources are increasing in the last decades. The significant attempts to protect the environment are concentrated on introducing substitutes to alter the plastic materials, with a developing classification of the natural materials. The quantity of projects proposing to develop the composites and polymers with natural materials is continuously increasing. The evolution of new materials made by natural fibers becomes a field of exceptional inquisitiveness, mainly due to the importance of advanced materials. Hence, polymers reinforced by natural fibers have fascinated too much attention among scientists in recent decades, owing to the demand for generating favorable environmental materials that have the ability to substitute the currently used materials [1–3].

Therefore, using extracted materials from nature as research topics become widespread around the world. Specifically, in the case of films and biocomposites, the use of biopolymers has come into view as a fascinating alternative. One of the common examples is the usage of chitosan provided by shells of shrimp and other similar species that has been studied for several years [4]. The biopolymers generally have been categorized into the two main groups. Those that extract from existing organisms and the other which require to be polymerized but extract from renewable and biodegradable resources. Based on this assortment, the first group consists of protein (collagen, gelatin, keratin, etc.), and polysaccharide (starch, chitosan, cellulose, etc.) and the second one is well illustrated by polylactic acid [5, 6]. In this study, two biopolymers from the first group have been merged to obtain a biocomposite. The chitosan derivates from polysaccharides and polyamide comes from proteins. Chitosan is constituted of β-(1,4)-2-amino-2-deoxy-D-glucose, a deacetylated product of chitin gained from crustacean and shrimp wastes.

Chitosan and its compounds have been widely studied owing to its low cost of production, biocompatibility, and biodegradability and because of its high usage in biomedical and cosmetic applications. In addition, this renewable biopolymer has significant potential as a packaging biopolymer owing to its high ability to form films [7–9].

On the other hand, Polyamide is a semi-crystalline thermoplastic biodegradable polymer that is used for several engineering applications. With all these interpretations, its heat distortion temperature is low, and it is water absorber for the presence of amide functional groups in its molecular chain, which exacerbates its mechanical properties, tribological properties and dimensional stability severely [10, 11]. So as to achieve to inhibit these shortages, chitosan nanoparticles, as a very well-known biocompatible and biodegradable material, has been blended with polyamide to obtain a polymer composite with distinguished properties [12, 13].

Electrospinning is a proper method to fabricate fibers with thickness ranging from micrometers to nanometers. The appreciable high surface area to volume, fine structure and high volume of porosity make electrospun nanofibers highly noteworthy to ultrasensitive sensors and growing importance in numerous applications [14]. The high application of polymeric semiconductors in biological sensors is the most significant reasons for the whole research and evolution of these biomaterials. During the past decades, many synthetic approaches have been proposed for the fabrication of one-dimensional semiconductor nanomaterials [15]. Especially, polyamide is one such polymer that has been studied the most owing to its ideal physical and mechanical properties [16]. Additionally, the functional and mechanical properties of these fibers can be improved by adding cross-linking agents such as chitosan [17]. Chitosan is a biodegradable natural nontoxic polymer obtained by deacetylation of chitin, maintaining chelating features and novel polycationic owing to the presence of active hydroxyl and amino functional groups. Consequently, the benefits of the biopolymer are taken from both chitosan and polyamide and by combining them into a nanocomposite by using the electrospinning method [18–20].

Recently, many efforts have been devoted to develop and characterize different types of polyamide/chitosan composites. Some important works have been done to investigate the different characterization of polyamide/chitosan as fire/flame retardant, various types of membrane, hybrid polymeric scaffolds for tissue engineering, antibacterial filters and etc. Latterly, Kundu et al. [21] deposit a few bilayers of chitosan and phytic acid to improve the flame retardant properties of polyamide fabrics. Furthermore, Plasma grafted polyamide has also been studied by grafting of chitosan oligomer on polyamide fibers exhibiting excellent potential for biocompatible and antibacterial fibers invention [22, 23]. Moreover, Some particular researches on the miscibility of polyamide with chitosan following dissolution in formic acid are also carried representing the high interaction between the molecular chains of both polymers [24, 25]. Gendi et al. [26] produced a membrane of polyamide-6/chitosan using the phase inversion method and used them for desalination. The result of this report indicated that adding chitosan to the polyamide/6 membrane has increased the salt refusal of the membrane because of attaching itself to the pores and diminishing the pore size of the membrane. As another application, polyamide-6 and chitosan have been used to form hybrid polymeric scaffolds for tissue engineering by

applying one-step electrospinning [27]. In addition, polyamide-6 is oxidized with chitosan using potassium persulfate and, then, chitosan is grafted into the polyamide/6 fabric to enhance antibacterial properties. The results exhibited an outstanding antibacterial rate of the fabric around 85% after 40 times of washing [28]. In another report, Polyamide-6/chitosan composite scaffolds are built by the electrospinning method, and the hydrophilicity and mechanical strength of the composite are enhanced by adding the chitosan as well as providing a suitable environment for osteoblast growth in vitro. Besides, biomineralization improved with the rising weight percentage of chitosan after incubation in a simulated body solution for 21 days [29]. Similar outcomes are reported in another research on the effect of Polyamide-6/chitosan nanofibers on osteoblast growth [30].It is additionally noted that for the extruded polyamide-6/chitosan composite films, the weak interaction between chitosan and polyamide matrix led to deteriorating mechanical properties of composite [31].

In this paper, the preparation of polyamide/chitosan nanocomposite by a single-solvent system with electrospinning method is reported. According to the literature, less attention is given to the high application potential of semiconducting polymers in biological and chemical sensors and it is one of the principal purposes for the investigation and development of these materials. The remarkable high surface-area-to-volume ratio, small diameter, and high porosity bring electrospun nanofibers highly interesting to ultrasensitive sensors and growing importance in many technological applications. This nanocomposite demonstrates uniform two-dimensional networks. The electrical and morphological characteristics of the prepared polyamide/chitosan nanocomposites are studied. Also, the crystallinity of the formed nanocomposite and their microstructure are investigated using field-emission scanning electron microscopy and X-ray diffraction. The influence of the nanofibers on the electrical features is studied by a semiconductor parameter analyzer as well.

2. Materials And Methods

2.1 Materials

Polyamide (181110 pellets, SIGMA-ALDRICH, Darmstadt, Germany) and chitosan powder (181110 pellets, SIGMA-ALDRICH, Darmstadt, Germany) are used in preparing the solution. The nanofibers are made by dissolving the chitosan powder and the pellets of polyamide in a single solvent of 80% formic acid (46.03 g/mol, 98–100%, Merck, Darmstadt, Germany) while they were mixed by the magnetic stirrer at 50°C for about 3 h. After preparing the polymer solution, they are cooled to approach room temperature. Polyamide (18 wt%) with various concentrations of chitosan with 0, 1, 3, and also 5 wt% is used to make the composite nanofiber mats.

2.2 Preparation of nanocomposite films

The prepared polymer solution is loaded into a 20 ml plastic syringe equipped with the polystyrene microtip (0.25 mm inner diameter and 15 mm length) attached to a steel nozzle (Gauge 18, Sigma - Aldrich), which is connected to the high-voltage power supply (R301 Meivac, USA). Electrospinning is carried out at a voltage of 20 kV and flow rate of 0.5 ml/h, respectively. A grounded iron drum is rotated at

a constant speed by a DC motor to roll up the fabricated nanofibers, which is held at a distance of 15 cm from the microtip like Fig. 1. The electrospinning process of all the solutions is performed in a close chamber for 2 h. During the procedure, the temperature and relative humidity are in the range of 20–25°C and 35% RH, respectively.

2.3 X-ray diffraction (XRD)

The relevant crystallinity of formed nanocomposite films are studied by Bruker D8 Venture diffractometer (Massachusetts, United States) in the diffraction angles range $2\theta = 10°$ and 60° by using Cu Kα radiation wavelength of 1.540A° with 0.025° as step size and 99 seconds time per step. The specimens are located in the sample holder, and analysis is performed in a static mode.

2.4 Thermogravimetric analysis (TGA)

Thermogravimetric analysis is carried out to evaluate the degradation characteristics of the polyamide/chitosan nanocomposite. The thermal stability of all specimens is determined by using a thermogravimetric analyzer (NETZSCH-Gerätebau GmbH, TG 209 F1 Libra®, Selb, Germany), under the nitrogen environment with a heating rate of 10°C/min.

2.5 Field-emission scanning electron microscopy (FE-SEM)

The microstructures of nanocomposite films are observed by field-emission scanning electron microscopy (FE-SEM). To study the morphology of polyamide/chitosan composite film, the prepared polyamide/chitosan nanocomposites are analyzed by (Schottky, SU5000, Hitachi, Japan) with an acceleration voltage of 20 KV. A plasma sputter is used to coat the surfaces of all the specimens by gold.

2.6 Current–voltage (I–V) characteristic and nanocomposite resistance

Silver metal is stuck on the surface of the films to have better ohmic contact. The current–voltage (I–V) characteristic is measured for the polyamide/chitosan nanocomposites by a semiconductor parameter analyzer (HP 4155B, United States). Also, the sheet resistance of all the prepared nanocomposites is achieved.

2.7 Fourier transform infrared spectroscopy (FT-IR)

FT-IR spectra are recorded to study the interactions between chitosan and polyamide using a JASCO FT/IR-4000 spectrometer (United States), with a resolution of 4 cm^{-1} in the range of 750–4000 cm^{-1}. The analysis is done for the polyamide matrix, polyamide/chitosan 1, 3 and 5 wt%.

3. Results And Discussion

3.1 Field-emission scanning electron microscopy (FE-SEM)

Figure 2 demonstrates the FE-SEM results of polyamide/chitosan nanocomposites for the various concentrations of chitosan with 1, 3 and 5 wt%, respectively. The electrospun nanofibers represent a completely smooth surface, randomly oriented nanofibers and uniform thickness of the fibers. As can be seen in the figure, a very precise arrangement of mesh-like nanofibers completely bound with the matrix is

observed. These ultrafine structures lead to a large surface area-to-volume ratio. The thickness of the nanofibers varies from 40 to 130 nm for the composites and it is thicker than the electrospun fibers of polyamide (Supplementary Information) which is obvious by comparing FE-SEM images of the composites and neat polyamide. The size of the nanofibers became one order smaller than the main fibers. The density of high aspect ratio fibers enhances with the raising of chitosan content. It is assumed that the form of the high surface-area-to-volume ratio of nanofibers is owing to the strongly applied voltage that is formed between two electrodes [32, 33].

Table 1 shows the statistics of fiber diameter based on the FE-SEM images of the prepared composites and the distributions of the fiber diameter histograms are presented in Fig. 2. According to the provided results, the mean fiber diameter (MFD) and related standard deviation (RSD) for the polyamide/chitosan 1 wt% are 70.94 nm and 5.48%, respectively. MFD value for the composite by increasing the content of chitosan up to 3 wt% is not changed significantly. As can be seen, by enhancing the content of chitosan up to 5 wt%, MFD has increased up to 88.12 nm. It can be notified that the thickness of the nanofibers is increased by enhancing the content of chitosan in the composite because. It can be concluded that an increase in polymer solution concentration results in higher viscoelastic forces which restrict stretching of polymer solution jets leading to the formation of thicker fibers.

Table 1

Statistics of fiber diameter.

C (wt%)	Min (nm)	Max (nm)	MFD (nm)	RSD (%)
1	52.38	97.87	70.94	5.48
3	42.99	104.04	70.07	5.26
5	58.91	127.48	88.12	3.77

3.2 X-ray diffraction (XRD)

The crystallinity of the prepared polyamide/chitosan nanocomposites are discriminated by XRD, and the achieved result is compared with the polyamide film. The XRD outcomes of the primitive and prepared polyamide/chitosan nanocomposite are given in Fig. 3. The diffraction pattern of polyamide nanofibers displayed a wide peak emerged at $2\theta = 20°$ which is related to the (100) crystal plane of polyamide. However, gradual broadening of this peak occurs when higher percentage of chitosan is added. Furthermore, the (100) 2θ peaks are shifted to the higher field as the content of chitosan is enhanced, which means that the d-spacings between the (100) plane are decreased as in the Bragg diffraction law, $2d\sin\theta = n\lambda$. It also confirms that the polymer structure of polyamide is modified by blending with chitosan which diminishes the hydrogen bond. Besides, it corresponds that the molecular chain packing rearrangement has occurred inside the blending films and successively distorted reformed structure appears after blending. As demonstrated in Fig. 3, the XRD pattern of prepared polyamide/chitosan

nanocomposite are formed by their characteristic peaks at 2θ = 20 and 25° attributed to the α_1(200) and α_2(200) phases, respectively [34]. Though, for the lower chitosan content (1 and 3 wt%) very weak peaks are perceived as recorded in the XRD results. The intensity is lightly enhanced with increasing of chitosan percent in the nanocomposites. In another hand, extra sharp peak at 2θ = 34° attributed to the characteristic of the γ phase [35]. The results proved the prosperous blending of chitosan in polyamide via the electrospinning method.

3.3 Thermogravimetric analysis (TGA)

Figure 4a demonstrates thermogravimetric analysis curves of the polyamide/chitosan 1 wt%, 3 wt% 5 wt%. The matrix and chitosan reinforced composites represent equal decomposition trends at diverse stages of treatment. Subsequently, Fig. 4b presents the first derivative thermogravimetric diagrams of the same specimens. The initial tracks of analysis of the samples revealed at temperatures under 100°C, which illustrates the loss of water and low molecular weights compounds [36]. The most important decomposition happened at nearly 300–500°C, indicating the decomposition of organic molecule of chitosan polymers. The analogous consequences are also reported by Shrestha et al.[29], who claimed that chitosan nanofibers started to decompose at temperatures above 200°C. The decomposition temperature of the polyamide/chitosan 5 wt% modified to a higher temperature compared to polyamide/chitosan 1 wt% and 3 wt%. According to figure of DTG, the principal decomposition temperature of the polyamide/chitosan 1 wt% is almost 260°C, whereas the decomposition temperature obtained by polyamide/chitosan 5 wt% raised to approximately 284°C. Also, the recorded decomposition temperature of the polyamide/chitosan 1 wt% and 5 wt% are each almost 245°C. The achieved outcomes are attributed to this fact that the chitosan compounded into the polyamide matrix strongly, making decomposition of the biocomposite arduous. Hence, better thermal stability is attained with chitosan as the reinforcement. Thermogravimetric analysis (particularly residue formation at 280°C) has explained that the attendance of inorganic–organic structures strongly intensifies the char formation. Besides, infrared spectroscopy has exposed that the combination of polyamide and chitosan is able to raise the formation of a char having an aromatic nature. Depending on the content of chitosan, the organic–inorganic combination are able to persuade the formation of a thermally stable aromatic char that protects the matrix from the application of a flame or different external heat fluxes. [37].

3.4 Current–voltage (I–V) characteristic and nanocomposite resistance

Figure 5a exhibits I–V characteristics of the polyamide/chitosan nanocomposite. Interestingly, while the chitosan content is raised, the current is magnified in comparison to the primitive polyamide. The creation of compacter ultrafine nanofibers with the summation of chitosan content presented a great advancement in I–V characteristics [38]. The surplus chitosan probably covered the fiber networks between polyamide/chitosan nanocomposites can be improved by the electrical pathways. Hence, the conductivity of the polyamide/chitosan 5 wt% demonstrates the maximum current of 0.3 nA. It is worthy to mention that the enhancement in the porosity of these nanocomposites can be used for the biosensor applications with advanced sensitivity and performance. Sheet resistances are measured from figures of the calculated resistance values versus the gaps between the metal contacts. Figure 5b presents the

sheet resistance of the prepared polyamide/chitosan nanocomposites with different chitosan volume percent. The sheet resistance is defined to be lowered from 118 to 20 × 10^9 Ω/□ with raising the chitosan volume from 0 to 5 wt%. As an important result, it is worth pointing out that the enhanced chitosan volume leads to a notable decrease in the sheet resistance in comparison to the pristine polyamide. The reduction in sheet resistance of chitosan loaded specimen can be associated with the highly compacter ultrafine nanofibers. The primary results completely proposed that the composition of ultrafine arrangements play a significant role on the electrical characteristics [39].

3.5 Fourier transform infrared spectroscopy (FT-IR)

One of the principal properties of polyamide or chitosan is the powerful interchain interaction which appears from the hydrogen bond between amide groups on neighboring chains. Ordinarily, some nanofillers have the ability to produce hydrogen bonds at interfaces with amide groups that can be precisely identified by FT-IR. Figure 6 displays two sections in the FT-IR spectra of polyamide/chitosan films nanocomposites. Figure 6A exhibits the range from 4000–2600 cm^{-1}. As can be seen, in this region, the spectrum associated with pristine polyamide film presents the band at 3400 cm^{-1} which is attributed to the hydrogen bond [40]. In the spectrum a-c, the principal vibrations associated with the chitosan structure are recognized in the region about 3300 cm^{-1} and these correspond to the range of amide bands [41]. Furthermore, the peak in 2950 cm^{-1} is allocated to the asymmetric vibration of the C-H of the methyl group [42, 43]. The nanocomposite films in this zone only display broad peaks which are associated with the signals of the stated peaks, discovered in chitosan and polyamide.

Figure 6B demonstrates the FT-IR spectra of pristine polyamide and polyamide/chitosan nanocomposites in the range from 1800–700 cm^{-1} [44]. As it is clear, in this range, the principal peaks attributed to the pristine polyamide films (spectrum a) are discovered, the peaks at 700–800 cm^{-1} correspond to the methylene structure, and the characteristic peaks between 1000–1150 cm^{-1} are associated to C–O bond stretching [45]. The specified peaks are accepted as principal references in the nanocomposite samples because those bands become visible at the equal wavenumber compared to the peaks seen in the polyamide/chitosan spectrum. A sharp shoulder is detected at 1020 cm^{-1} that corresponds to chemical bond of C–O–C in nanocomposites samples with hydrogen bonds. Also in Fig. 6B, the principal bands associated with chitosan are also perceived, the peak at 1630 cm^{-1} is attributed to the interaction of C = O group and the bands at 1510 cm^{-1} and 1530 cm^{-1} correspond to bending of N-H groups [46].

4. Conclusions

Polyamide/chitosan nanocomposites are successfully fabricated using the electrospinning procedure with high aspect ratio structure. These electrospun nanofibers are perceived with similar thicknesses along their lengths. The polyamide/chitosan nanocomposites with diameters of about 40–130 nm are attached in the main matrix. Characterization of the prepared polyamide/chitosan nanocomposite by Fourier transform infrared spectroscopy exhibited that the amide functional groups concluded polyamide nanofillers with a stable composition. The polyamide/chitosan blended represented a single melting peak

approximately at 250°C. Thermogravimetric analysis indicated that the origin disintegration temperature for polyamide/chitosan nanocomposites is perceived to be in the range from 100 to 350°C. The electrical conductivity of nanocomposite enhanced with raising of chitosan volume. The electrical properties of the polyamide/chitosan nanocomposite improved with increasing content of chitosan, which is associated with the production of nanofibers. The resistance of the sheet is measured to be reduced with increasing of chitosan volume. The important enhancement in the electrical characteristics of the mentioned biodegradable composite can be appropriated for quite promising nanotechnological applications.

Declarations

Acknowledgment

This work is based on the research supported by the Iran Nanotechnology Initiative Council (85106066). The authors are also thankful for the support provided by CAPES - Brazilian Foundation for the Advancement of Graduate Studies and FAPERJ - Foundation for Research Development of the State of Rio de Janeiro.

References

1. Chen Z, Li T, Yang Y, et al (2004) Mechanical and tribological properties of PA/PPS blends. Wear 257:696–707. https://doi.org/10.1016/j.wear.2004.03.013

2. Fazeli M, Keley M, Biazar E (2018) Preparation and characterization of starch-based composite films reinforced by cellulose nanofibers. Int J Biol Macromol 116:272–280. https://doi.org/10.1016/j.ijbiomac.2018.04.186

3. Fazeli M, Simão RA (2019) Preparation and characterization of starch composites with cellulose nanofibers obtained by plasma treatment and ultrasonication. Plasma Process Polym 1–10. https://doi.org/10.1002/ppap.201800167

4. Pellá MCG, Lima-Tenório MK, Tenório-Neto ET, et al (2018) Chitosan-based hydrogels: From preparation to biomedical applications. Carbohydr. Polym. 196:233–245

5. Zarei H, Nazari M, Koushali AG (2020) Effect of interleaved composite nanofibrous mats on quasi-static and impact properties of composite plate. Iran Polym J (English Ed. https://doi.org/10.1007/s13726-020-00845-1

6. Fong D, Hoemann CD (2018) Chitosan immunomodulatory properties: perspectives on the impact of structural properties and dosage. Futur Sci OA 4:FSO225. https://doi.org/10.4155/fsoa-2017-0064

7. Ren L, Yan X, Zhou J, et al (2017) Influence of chitosan concentration on mechanical and barrier properties of corn starch/chitosan films. Int J Biol Macromol 105:1636–1643. https://doi.org/10.1016/j.ijbiomac.2017.02.008

8. Moghaddam S, Taghi Khorasani M, Hosseinkazemi H, et al (2016) Fabrication of polyhydroxybutyrate (PHB)/γ-Fe_2O_3 nanocomposite film and its properties study. J Biomater Sci Polym Ed 27:793–804. https://doi.org/10.1080/09205063.2016.1143320

9. Florez JP, Fazeli M, Simão RA (2019) Preparation and characterization of thermoplastic starch composite reinforced by plasma-treated poly (hydroxybutyrate) PHB. Int J Biol Macromol 123:609–621. https://doi.org/10.1016/j.ijbiomac.2018.11.070

10. Jun B-M, Kim SH, Kwak SK, Kwon Y-N (2018) Effect of acidic aqueous solution on chemical and physical properties of polyamide NF membranes. Appl Surf Sci 444:387–398. https://doi.org/10.1016/J.APSUSC.2018.03.078

11. Jordanov I, Kolibaba TJ, Lazar S, et al (2020) Flame suppression of polyamide through combined enzymatic modification and addition of urea to multilayer nanocoating. J Mater Sci 55:15056–15067. https://doi.org/10.1007/s10853-020-05074-8

12. Dotto GL, Santos JMN, Tanabe EH, et al (2017) Chitosan/polyamide nanofibers prepared by Forcespinning®technology: A new adsorbent to remove anionic dyes from aqueous solutions. J Clean Prod 144:. https://doi.org/10.1016/j.jclepro.2017.01.004

13. Selvi J, Parthasarathy V, Mahalakshmi S, et al (2020) Optical, electrical, mechanical, and thermal properties and non-isothermal decomposition behavior of poly(vinyl alcohol)–ZnO nanocomposites. Iran Polym J (English Ed 29:411–422. https://doi.org/10.1007/s13726-020-00806-8

14. Tas M, Xu F, Ahmed I, Hou X (2020) One-step fabrication of superhydrophobic P(VDF-co-HFP) nanofibre membranes using electrospinning technique. J Appl Polym Sci 137:. https://doi.org/10.1002/app.48817

15. Fang H, Li D, Wu F, et al (2020) In situ Polymerization of Polyamide 6/Boron Nitride Composites to Enhance Thermal Conductivity and Mechanical Properties via Boron Nitride Covalently Grafted Polyamide 6. Polym Eng Sci 60:710–716. https://doi.org/10.1002/pen.25329

16. Li Y, Yang G (2004) Studies on molecular composites of polyamide 6/polyamide 66. Macromol Rapid Commun 25:1714–1718. https://doi.org/10.1002/marc.200400262

17. Falamarzpour P, Behzad T, Zamani A (2017) Preparation of nanocellulose reinforced chitosan films, cross-linked by adipic acid. Int J Mol Sci 18:. https://doi.org/10.3390/ijms18020396

18. Gutiérrez TJ (2017) Chitosan Applications for the Food Industry. In: Chitosan. pp 183–232

19. Sun K, Li ZH (2011) Preparations, properties and applications of chitosan based nanofibers fabricated by electrospinning. Express Polym Lett 5:342–361. https://doi.org/10.3144/expresspolymlett.2011.34

20. Fazeli M, Simão RA (2018) The Effect of Cellulose Nanofibers on the Properties of Starch Biopolymer. Macromol Symp 380:1800110. https://doi.org/10.1002/masy.201800110

21. Kundu CK, Li Z, Song L, Hu Y (2020) An overview of fire retardant treatments for synthetic textiles: From traditional approaches to recent applications. Eur. Polym. J. 137

22. Mccord MG, Hwang YJ, Hauser PJ, et al (2002) Modifying Nylon and Polypropylene Fabrics with Atmospheric Pressure Plasmas. Text Res J 72:491–498. https://doi.org/10.1177/004051750207200605

23. Fazeli M, Simão RA (2019) Preparation and characterization of starch composites with cellulose nanofibers obtained by plasma treatment and ultrasonication. Plasma Process Polym 16:. https://doi.org/10.1002/ppap.201800167

24. Ko MJ, Jo WH, Kim HC, Lee SC (1997) Miscibility of chitosans/polyamide 6 blends. Polym J 29:997–1001. https://doi.org/10.1295/polymj.29.997

25. González V, Guerrero C, Ortiz U (2000) Chemical structure and compatibility of polyamide-chitin and chitosan blends. J Appl Polym Sci 78:850–857. https://doi.org/10.1002/1097-4628(20001024)78:4<850::AID-APP190>3.0.CO;2-N

26. EL-Gendi A, Deratani A, Ahmed SA, Ali SS (2014) Development of polyamide-6/chitosan membranes for desalination. Egypt J Pet 23:169–173. https://doi.org/10.1016/j.ejpe.2014.05.003

27. Sanchez-Salvador JL, Balea A, Monte MC, et al (2021) Chitosan grafted/cross-linked with biodegradable polymers: A review. Int. J. Biol. Macromol. 178:325–343

28. Shi Z (2014) Grafting chitosan oxidized by potassium persulfate onto Nylon 6 fiber, and characterizing the antibacterial property of the graft. J Polym Res 21:534–539. https://doi.org/10.1007/s10965-014-0534-0

29. Shrestha BK, Mousa HM, Tiwari AP, et al (2016) Development of polyamide-6,6/chitosan electrospun hybrid nanofibrous scaffolds for tissue engineering application. Carbohydr Polym 148:107–114. https://doi.org/10.1016/j.carbpol.2016.03.094

30. Nirmala R, Navamathavan R, Kang HS, et al (2011) Preparation of polyamide-6/chitosan composite nanofibers by a single solvent system via electrospinning for biomedical applications. Colloids Surfaces B Biointerfaces 83:173–178. https://doi.org/10.1016/j.colsurfb.2010.11.026

31. Lago MA, Sendón R, de Quirós ARB, et al (2014) Preparation and Characterization of Antimicrobial Films Based on Chitosan for Active Food Packaging Applications. Food Bioprocess Technol 7:2932–2941. https://doi.org/10.1007/s11947-014-1276-z

32. Wang L (2008) Functional Nanofibre: Enabling Material for the Next Generation Smart Textiles. J Fiber Bioeng Informatics 1:81–92. https://doi.org/10.3993/jfbi09200801

33. Ramakrishna S, Fujihara K, Teo WE, et al (2006) Electrospun nanofibers: Solving global issues. Mater Today 9:40–50. https://doi.org/10.1016/S1369-7021(06)71389-X

34. Uragami T (2019) Chitin and Chitosan Derivative Membranes in Resources, Energy, Environmental and Medical Field. pp 175–269

35. Zhang H, Li S, Branford White CJ, et al (2009) Studies on electrospun nylon-6/chitosan complex nanofiber interactions. Electrochim Acta 54:5739–5745. https://doi.org/10.1016/j.electacta.2009.05.021

36. Kundu CK, Wang X, Rahman MZ, et al (2020) Application of Chitosan and DOPO derivatives in fire protection of polyamide 66 textiles: Towards a combined gas phase and condensed phase activity. Polym Degrad Stab 176:. https://doi.org/10.1016/j.polymdegradstab.2020.109158

37. Chrzanowska E, Gierszewska M, Kujawa J, et al (2018) Development and characterization of polyamide- supported chitosan nanocomposite membranes for hydrophilic pervaporation. Polymers (Basel) 10:. https://doi.org/10.3390/polym10080868

38. Singh RK, Lye SW, Miao J (2020) Measurement of impact characteristics in a string using electrospun PVDF nanofibers strain sensors. Sensors Actuators, A Phys 303:. https://doi.org/10.1016/j.sna.2020.111841

39. Thomas M, Rajiv S (2020) Grafted PEO polymeric ionic liquid nanocomposite electrospun membrane for efficient and stable dye sensitized solar cell. Electrochim Acta 341:. https://doi.org/10.1016/j.electacta.2020.136040

40. Osman Z, Arof AK (2003) FTIR studies of chitosan acetate based polymer electrolytes. Electrochim Acta 48:993–999. https://doi.org/10.1016/S0013-4686(02)00812-5

41. Cárdenas G, Miranda SP (2004) FTIR and TGA studies of chitosan composite films. J Chil Chem Soc 49:291–295. https://doi.org/10.4067/S0717-97072004000400005

42. Maillo J, Pages P, Vallejo E, et al (2005) FTIR spectroscopy study of the interaction between fibre of polyamide 6 and iodine. Eur Polym J 41:753–759. https://doi.org/10.1016/j.eurpolymj.2004.11.030

43. Garcia EE, Freitas DFS, Cestari SP, et al (2020) Zirconium phosphate changing hygroscopicity of polyamide-6 in nanocomposites PA-6/ZrP. J Therm Anal Calorim 139:293–303. https://doi.org/10.1007/s10973-019-08396-1

44. Vasanthan N, Salem DR (2001) FTIR spectroscopic characterization of structural changes in polyamide-6 fibers during annealing and drawing. J Polym Sci Part B Polym Phys 39:536–547. https://doi.org/10.1002/1099-0488(20010301)39:5<536::AID-POLB1027>3.0.CO;2-8

45. Pramoda KP, Chung TS, Liu SL, et al (2000) Characterization and thermal degradation of polyimide and polyamide liquid crystalline polymers. Polym Degrad Stab 67:365–374.

https://doi.org/10.1016/S0141-3910(99)00138-X

46. Mehrabzadeh M, Kamal MR (2002) Polymer-clay nanocomposites based on blends of polyamide-6 and polyethylene. Can J Chem Eng 80:1083–1092. https://doi.org/10.1002/cjce.5450800610

Figures

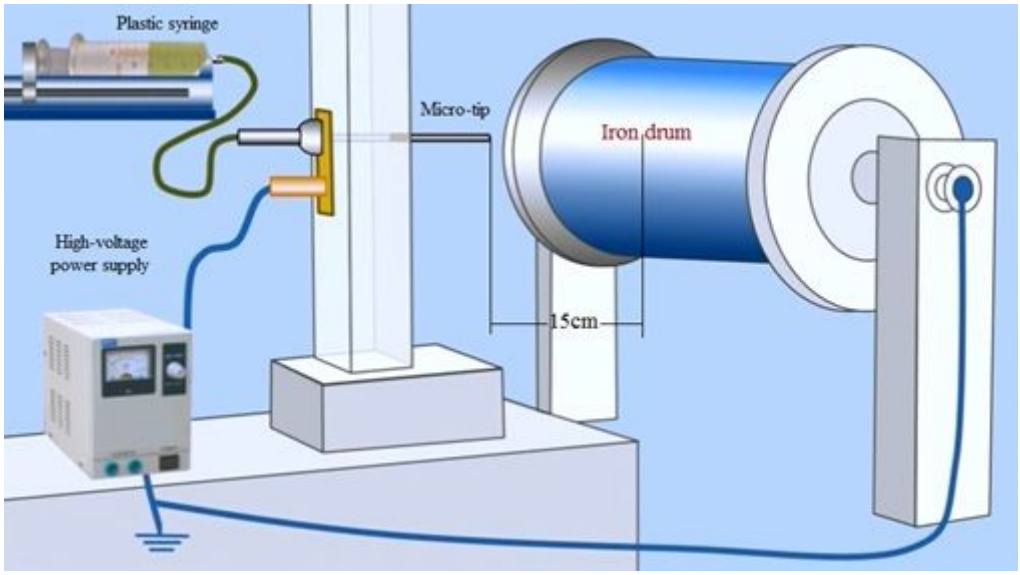

Figure 1

Schematic of the electrospinning process.

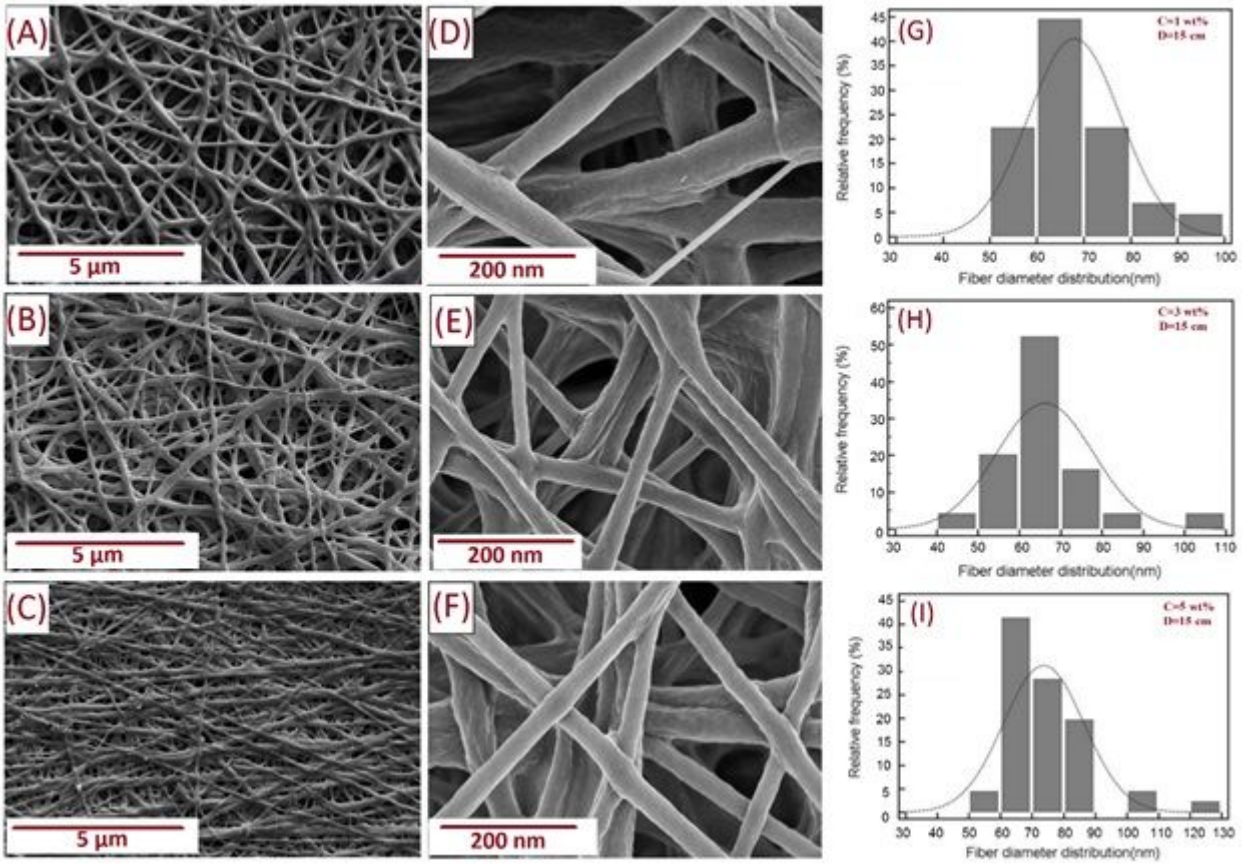

Figure 2

FE-SEM images of electrospun polyamide/chitosan composite nanofibers with different wt% of chitosan (a,d) 1, (b,e) 3, (c,f) 5 and histograms of electrospun fiber diameter distribution with different wt% of chitosan (g) 1, (h) 3, and (i) 5.

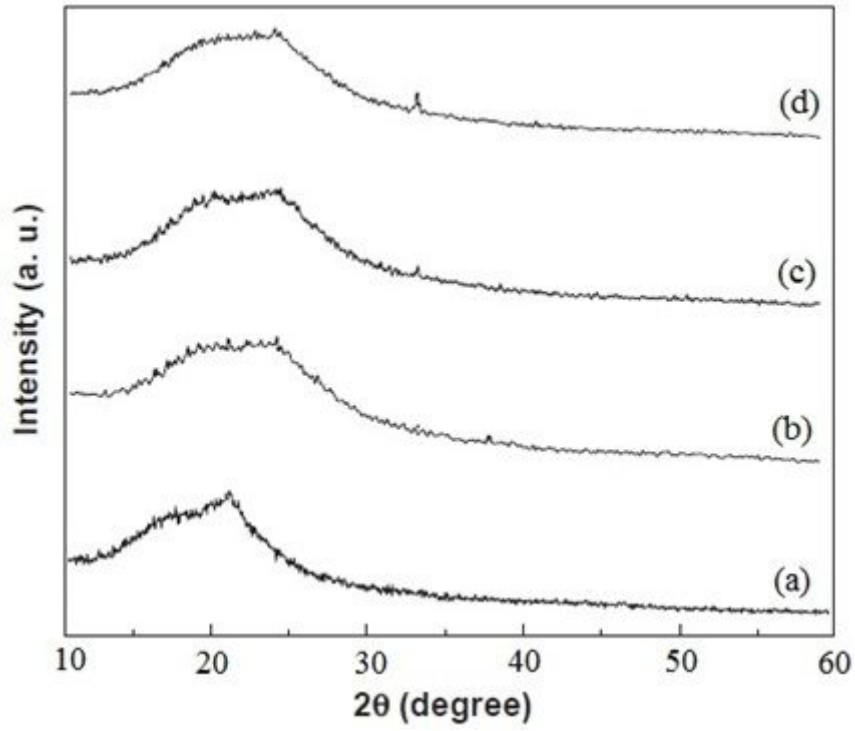

Figure 3

XRD graph of polyamide/chitosan nanocomposites with various chitosan content of (a) 0 wt%, (b) 1 wt%, (c) 3 wt% and (d) 5 wt%.

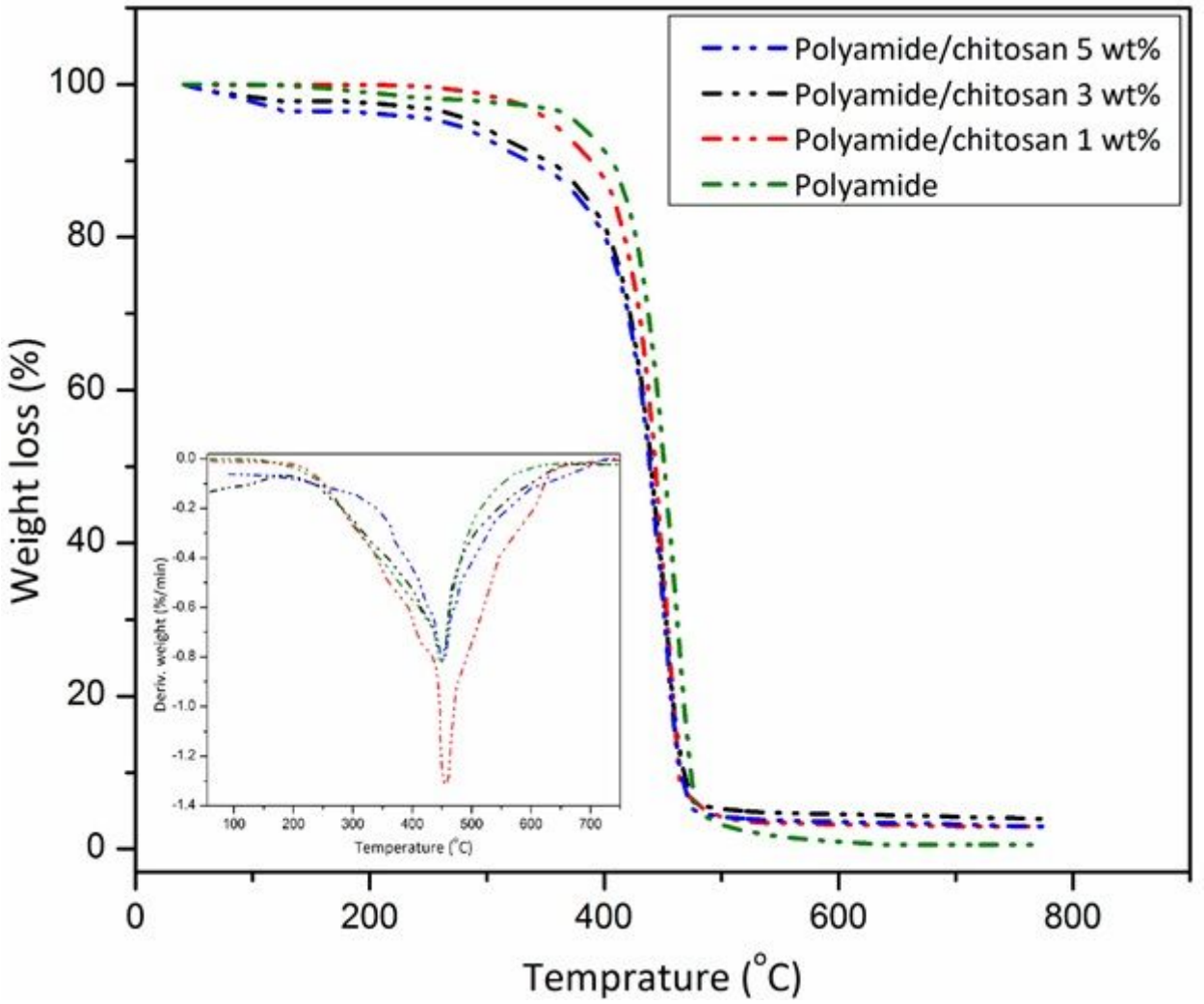

Figure 4

TGA and DTG curves for the polyamide/chitosan nanocomposite.

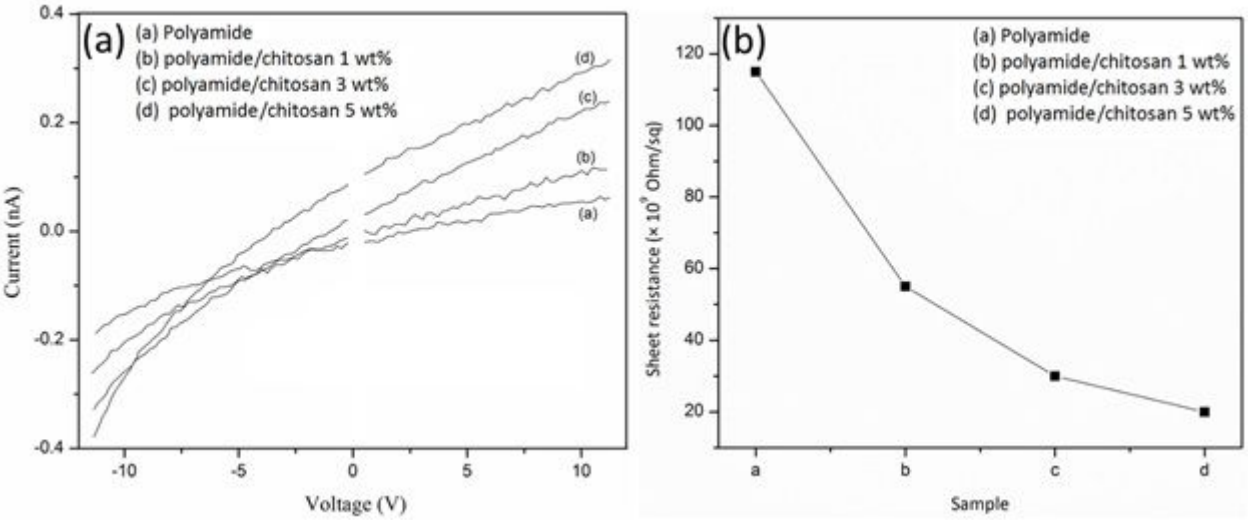

Figure 5

I–V characteristics (a) and sheet resistance (b) of polyamide/chitosan samples.

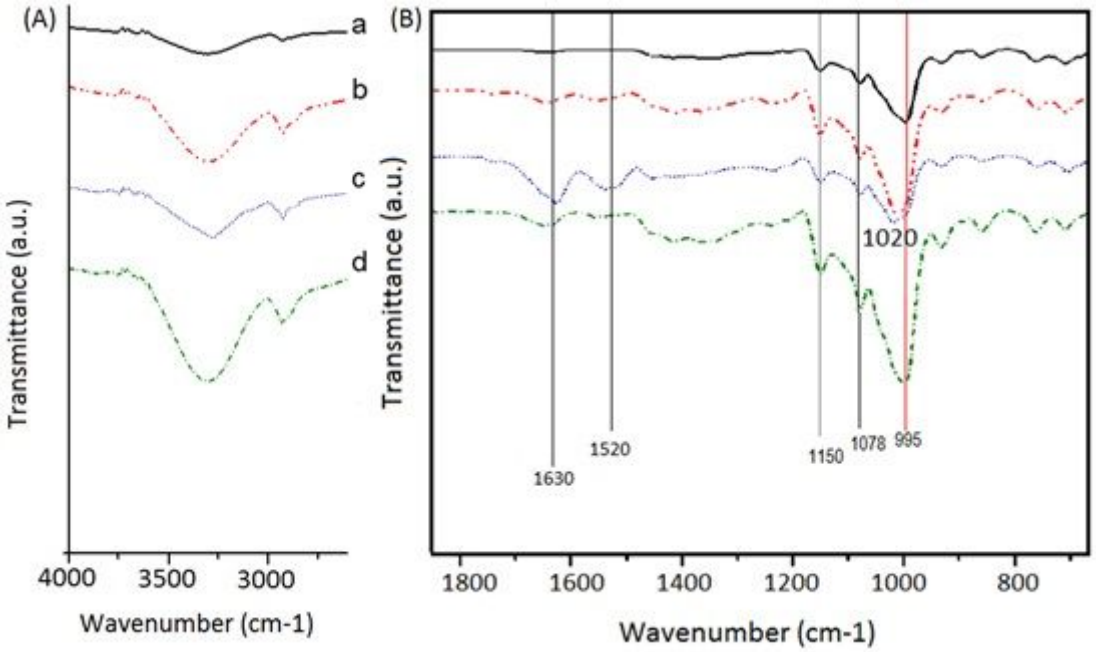

Figure 6

FT-IR spectra of pristine polyamide (a), polyamide/chitosan 1 wt% (b), polyamide/chitosan 3 wt% (c) and polyamide/chitosan 5 wt% (d).